Journal of Hazardous Materials 186 (2011) 1118–1123

Contents lists available at ScienceDirect

Journal of Hazardous Materials

journal homepage: www.elsevier.com/locate/jhazmat

Removal of rhodamine B using iron-pillared bentonite

Mei-Fang Hou[a,b], Cai-Xia Ma[c], Wei-De Zhang[a,*], Xiao-Yan Tang[b], Yan-Ning Fan[b], Hong-Fu Wan[b]

[a] School of Chemistry and Chemical Engineering, South China University of Technology, Guangzhou 510641, China
[b] Guangdong Key Laboratory of Agricultural Environment Pollution Integrated Control, Guangdong Institute of Eco-environmental and Soil Sciences, Guangzhou 510650, China
[c] Department of Material Invention, State Intellectual Property Office of the People's Republic of China, Beijing 100088, China

ARTICLE INFO

Article history:
Received 16 September 2010
Received in revised form
22 November 2010
Accepted 26 November 2010
Available online 3 December 2010

Keywords:
Clay
Bentonite
Iron pillaring
Rhodamine B
Adsorption

ABSTRACT

The iron-pillared bentonite (Fe-Ben) was prepared by ion-exchange using the natural bentonite (GZ-Ben) from Gaozhou, China, at room temperature without calcination. Both Fe-Ben and GZ-Ben were characterized by X-ray diffraction, N_2 adsorption and Fourier transform infrared spectroscopy. The results show that the $d(0\,0\,1)$ value and surface area of the bentonite material increased after iron pillaring. Fe-Ben adsorbed much more Rhodamine B (RhB) than GZ-Ben, which can be ascribed to the special surface properties and large surface area of Fe-Ben. The optimum pH value for the adsorption of RhB on Fe-Ben is 5.0. The adsorption of RhB onto Fe-Ben can be well described by the pseudo-second-order kinetic model and the intraparticle diffusion kinetic model. The adsorption isotherm of RhB onto Fe-Ben matches well with the Langmuir model.

1. Introduction

Dyes and pigments are widely used in the textile, paper, plastic, leather, guest–host liquid crystal displays, solar cells, food and mineral processing industries. The effluents containing dyes and pigments have been paid great attention in recent years since they can cause environmental problems. The removal methods of dyes include physical adsorption, chemical degradation, biological degradation, photodegradation or the synergic treatments of different methods [1–5]. Among them, physical adsorption by clay adsorbent plays an important role in the removal of dyes and pigments [6,7]. Several researches have shown that natural bentonite and iron-pillared bentonite represent the innovative and promising classes of clay adsorbent materials for removal of dyes. In replacing the natural inorganic exchange cations by metal polyhydroxy cations, especially by iron polyhydroxy cation, bentonite can be modified to promote adsorption and degradation of pollutants [8–11].

Rhodamine B (RhB) is a highly water soluble, basic dye of the xanthene class and is widely used in biological, analytical, and optical sciences [12]. It is reported that RhB is harmful to the environment [13]. The removal of this basic dye by bentonite-based materials is a promising alternative [14]. In this paper, the iron-pillared bentonite was prepared and the adsorption of RhB onto the iron-pillared bentonite was investigated. For comparison, the adsorption of RhB onto the natural bentonite was also investigated. The adsorption mechanism of RhB on these adsorbents was discussed.

2. Materials and methods

2.1. The natural bentonite and chemicals

The natural bentonite from Gaozhou in Guangdong province, China was named as GZ-Ben, which was ground to pass 300 mesh sieves and then dried at 373 K for 12 h. The chemical composition of GZ-Ben is summarized in Table 1. The target dye pollutant rhodamine B (RhB) was obtained from Guangzhou Chemical Co., China. $Fe(NO_3)_3{\bullet}9H_2O$, HCl and NaOH were purchased from Shanghai Chemical Co., China. All chemicals were of analytical grade and used as received. In the experiments, deionized water was used for preparing the solutions and suspensions.

2.2. Preparation of bentonite materials

The iron-pillared bentonite materials were prepared with the following procedure. Firstly, the pre-dried GZ-Ben was modified to Na-bentonite using the method reported in reference [14], and then 5 g Na-bentonite was dispersed into 200 mL deionized water. Secondly, the pillaring agents were prepared by adding 1.0 M NaOH into 100 mL, 1.0 M $Fe(NO_3)_3$ solution with molar ratio of $[Fe]/[OH^-]$ 1:1 under vigorous stirring, and then continued to stir for 24 h fol-

* Corresponding author. Tel.: +86 20 8711 4099; fax: +86 20 8711 4099.
E-mail address: zhangwd@scut.edu.cn (W.-D. Zhang).

0304-3894/$ – see front matter © 2010 Elsevier B.V. All rights reserved.
doi:10.1016/j.jhazmat.2010.11.110

Table 1
The CEC value of GZ-Ben and its main chemical composition.

CEC* (meq. per 100 g of bentonite)	SiO_2 (%)	Al_2O_3 (%)	Fe_2O_3 (%)	TiO_2 (%)	MgO (%)	CaO (%)	Na_2O (%)
95.48	68.73	14.61	0.63	0.10	4.48	1.11	0.31

lowed by aging at 298 K for 2 d. Thirdly, the prepared pillaring agent of 50 mL was added into the prepared Na-bentonite suspension of 100 mL and aged at 373 K for 2 d, and then the iron-pillared bentonite powder was collected, washed by deionized water for several times, dried in an oven under air at 305 K for 24 h and ground for use. The prepared iron-pillared bentonite was named as Fe-Ben. The iron content of Fe-Ben was up to 12.7%.

2.3. Characterization

The X-ray powder diffraction (XRD) measurement was carried out by a Rigaku D/max 2500 diffractometer using Cu Kα radiation (λ = 0.15418 nm); the accelerating voltage was 30 kV and the emission current was 30 mA. The Fourier transform infra-red (FTIR) spectra were recorded as KBr pellets in the spectral range 4000–400 cm^{-1} on a Perkin–Elmer 1725X FTIR spectrometer. The specific surface area and pore distribution of the prepared samples were investigated by N_2 adsorption using a Micromeritics ASAP 2020 instrument.

2.4. Adsorption experiments

At the reported optimum pH 7.0 for adsorption of RhB onto montmorillonite [14], comparison between Fe-Ben and GZ-Ben for adsorption of RhB was investigated in the following experiments. 0.03 g adsorbent was added into 20 mL solution of 10 mg/L RhB at pH 7.0, and then the mixture was shaken in a glass vial sealed with Teflon-lined screw caps at 298 ± 1 K for 1 h. Then, the suspensions were taken and separated by centrifugation at 4500 rpm for 30 min to get the supernatant for analysis. All the adsorption experiments were conducted in dark.

The experiments were also carried out for selecting the optimum pH for the adsorption of RhB onto Fe-Ben. The initial pH value in the solution of RhB was adjusted by 1.0 M HCl and 1.0 M NaOH. 0.03 g adsorbent was added into 200 mL solution of RhB with the initial concentration of 20 mg/L at different pH (3.0–11.0) and then the mixture was stirred in a flask at 298 ± 1 K for 10 min. The optimum pH was selected for favoring the adsorption of RhB and then used in the following kinetic and isotherm experiments.

The concentration of RhB was quantified by UV–Visible absorption spectrophotometry (TU1800-PC, Beijing). The measurements were carried out right after each sampling. Reaction solution was diluted 5 times before recording spectra in the most prominent absorbance region. The concentration of RhB in the solution at different pH values was determined with the standard curve at the same pH value. The pH value was detected by a pH meter (pHS-3, Shanghai, China).

The leaching of iron cation from Fe-Ben during the experiments under different pH was monitored colorimetrically according to the 1,10-phenanthroline method [15] with UV–Visible spectrophotometry (TU1800-PC, Beijing).

2.5. Adsorption kinetics

The batch experiments were carried out for investigating the adsorption kinetics of RhB onto Fe-Ben at room temperature under different conditions, including the initial concentration of RhB (10–50 mg/L) and the Fe-Ben dose (0.075–0.50 g/L). For all experiments, Fe-Ben was added into the 200 mL solution of RhB at the optimum pH.

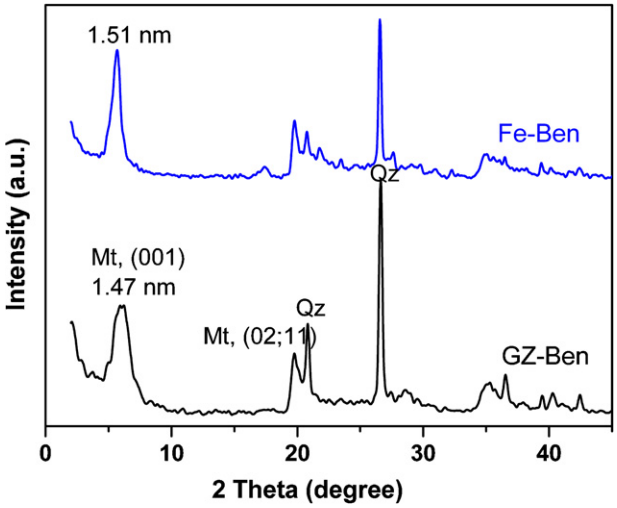

Fig. 1. The XRD patterns of Fe-Ben and GZ-Ben (M: montmorillonite; Qz: quartz).

2.6. Adsorption isotherms

Batch experiments were conducted to determine the adsorption isotherms of RhB in the aqueous solutions as follows: 0.01 g Fe-Ben was added into 20 mL solution of RhB, and then the mixture was shaken in a glass vial sealed with Teflon-lined screw caps at 298 ± 1 K for 24 h to reach the adsorption equilibrium at the optimum pH.

3. Results and discussion

3.1. Characterization of adsorbents

The XRD patterns of GZ-Ben and Fe-Ben were shown in Fig. 1. For the GZ-Ben, peaks at 2θ values of 6.1° and 19.8° are assigned to the (0 0 1) and (0 2, 1 1) reflections of montmorillonite [16], and the peaks at 2θ value of 20.8° and 26.6° are from quartz [17]. After iron pillaring, the *d*(0 0 1) reflection for basal spacing of the natural bentonite shifted from 1.47 nm (GZ-Ben) to 1.51 nm (Fe-Ben). It is noticed that no new major peaks appeared at 14.2° to γ-FeOOH, 21.2° to α-FeOOH, 26.7° to β-FeOOH, 33.2° to hematite (Fe_2O_3) and 35.4° to magnetite (Fe_3O_4) [18], which suggested that there is no iron oxides or hydroxides in the Fe-Ben. The BET surface area and pore volume of the bentonite materials obviously increased after iron pillaring (Table 2). It can be derived that poly-hydroxyl ferric intercalated in the interspaces of GZ-Ben and iron-pillared bentonite (Fe-Ben) of high surface area was prepared successfully at room temperature.

The FTIR results of GZ-Ben and Fe-Ben show that Al–OH–Al stretching band at 3637 cm^{-1} and bending band at 913 cm^{-1} should be characteristic of bentonite (Fig. 2) [19]. Bands at 3412 cm^{-1} (H–O–H stretching) and 1639 cm^{-1} (H–O–H bending) contribute to the adsorbed water. The weak band at 1384 cm^{-1} of Fe-Ben can

Table 2
The basal spacing *d*(0 0 1), BET surface area and pore volumes of Fe-Ben and GZ-Ben, and the removal of RhB onto these adsorbents.

Materials	*d*(0 0 1) (nm)	BET (m^2/g)	Pore volume (μL/g)	RhB removal (%)
Fe-Ben	1.51	36.8	42	>99
GZ-Ben	1.47	7.5	28	19

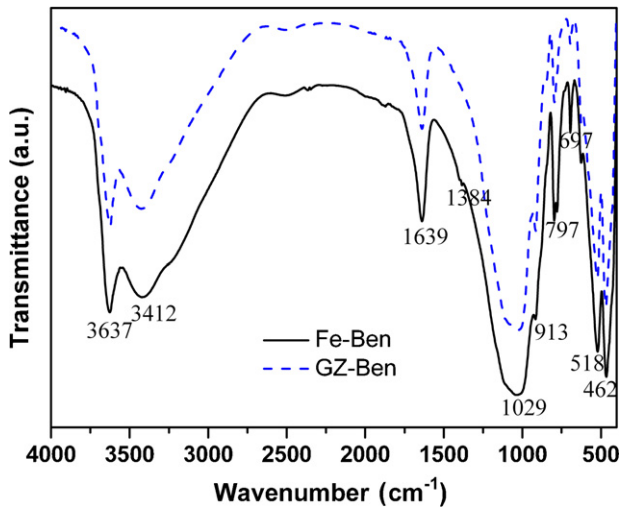

Fig. 2. The FTIR spectra of Fe-Ben and GZ-Ben.

be ascribed to the stretching of NO_3^-. The strong band at 1029 cm^{-1} is assigned to the Si–O–Si stretching vibration. The bands at 797, 697, 518 and 462 cm^{-1} are attributable to quartz [20].

Table 2 shows that the adsorption of RhB onto Fe-Ben is much better than that onto GZ-Ben, which can be attributed to the much larger surface area and pore volume of Fe-Ben.

3.2. Effect of pH on adsorption of RhB onto Fe-Ben

It is well known that the adsorption of dye onto adsorbent is highly dependent on the pH value of the solution, which influences the structure of dye and the surface properties of adsorbent [1,14,21–23]. The experiments were carried out to investigate the effect of pH value of the reaction solution on the adsorption of RhB onto Fe-Ben. At 10 min, the removal of RhB was up to 98%, reaching the highest degree at pH 5.0 in a system containing 20 mg/L RhB and 0.15 g/L Fe-Ben (Fig. 3). The optimum pH for different dyes being adsorbed onto different clay adsorbents is various [1,21,24]. Since the structure of RhB at different pH is diverse, its adsorption is complicated [23]. As for the natural bentonite, a significantly high electrostatic attraction exists between the negatively charged surface of the adsorbent and positively charged dye at pH 7.0 [1]. After iron pillaring, more surface hydroxyl groups present on the Fe-Ben than on natural bentonite. The surface hydroxyl groups of Fe-Ben are also pH-sensitive. Thus, the optimum pH for the natural bentonite and iron pillared bentonite is different. The adsorption mechanism of RhB onto the Fe-Ben at different pH will be discussed later in details.

The experimental results also show that there was little leaching of iron cations from Fe-Ben under different pH, so the leaching of iron cations was omitted in the following experiments. Thus, the following experiments were conducted at pH 5.0 for the adsorption of RhB onto the Fe-Ben.

3.3. Adsorption kinetics of RhB

To investigate the effect of different initial concentration of RhB and different adsorbent dosage on the adsorption kinetics of RhB by Fe-Ben, a series of adsorption experiments were carried out at pH 5.0 and 298 K.

The adsorption kinetics can be described by the pseudo-first-order kinetic model and the pseudo-second-order kinetic model [1,24]. The pseudo-first-order equation is generally expressed as Eq. (1):

$$\frac{1}{q_t} = \left(\frac{k_1}{q_1}\right)\left(\frac{1}{t}\right) + \frac{1}{q_1} \quad (1)$$

where q_1 and q_t are the equilibrium adsorption capacity (mg/g) and the adsorption capacity at time t, respectively; k_1 is the rate constant of pseudo-first-order adsorption (min^{-1}). The plot of $1/q_t$ vs. $1/t$ should give a linear relationship from which k_1 and q_1 can be determined from the slope and intercept of the plot, respectively. The pseudo-second-order equation is expressed as Eq. (2) [1,24]:

$$\frac{t}{q_t} = \frac{1}{k_2 q_2^2} + \frac{1}{q_2}t \quad (2)$$

where q_1 and q_t are the equilibrium adsorption capacity (mg/g) and the adsorption capacity at time t, respectively; k_2 is the rate constant of pseudo-second-order adsorption kinetic (g/mg min) and there is a linear relationship between t/q_t and t, q_2 and k_2 can be determined from the slope and intercept of the plot of t/q_t vs. t, respectively.

The intraparticle diffusion kinetic of RhB onto Fe-Ben was also investigated with the following model (Eq. (3)) [24]:

$$q_t = k_p t^{0.5} + C \quad (3)$$

where k_p is the intraparticle diffusion rate constant [mg/(g $min^{0.5}$)], C is a constant. k_p and C can be derived from the plot of q_t vs. $t^{0.5}$.

As shown in Figs. 4 and 5, the adsorption rate of RhB onto Fe-Ben decreased with the increasing of the initial concentration of RhB

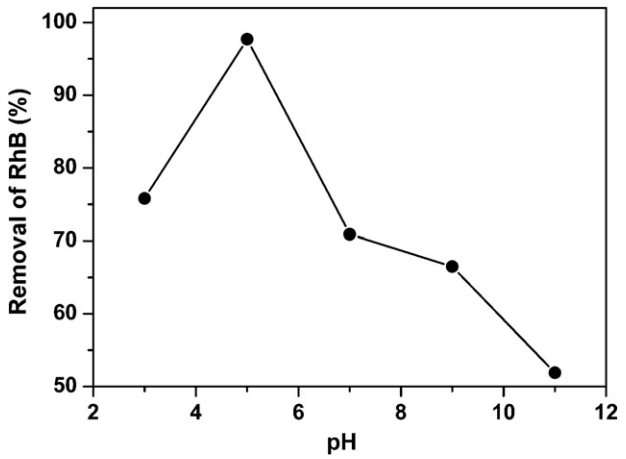

Fig. 3. The effect of pH value on the adsorption of RhB by Fe-Ben at 298 K (RhB: 20 mg/L; Fe-Ben: 0.15 g/L).

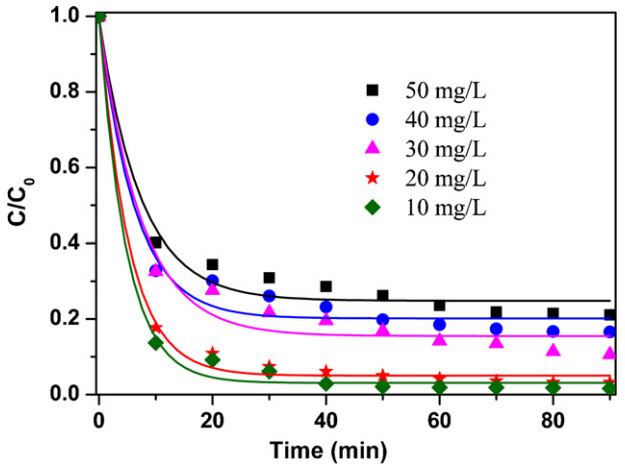

Fig. 4. The effect of initial concentration of RhB on its adsorption onto Fe-Ben at pH 5.0 and 298 K.

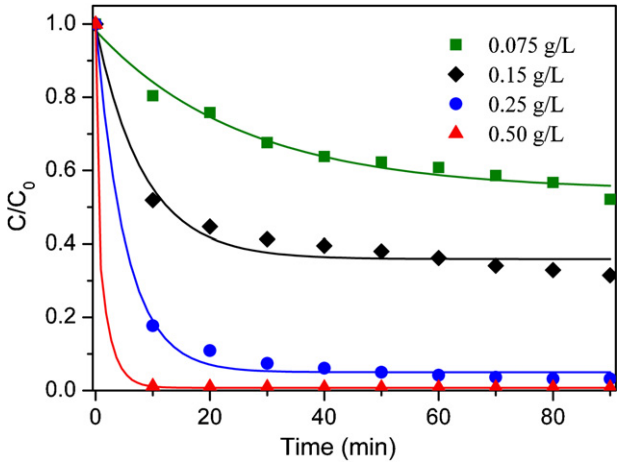

Fig. 5. The effect of Fe-Ben dosage on the adsorption of RhB at pH 5.0 and 298 K.

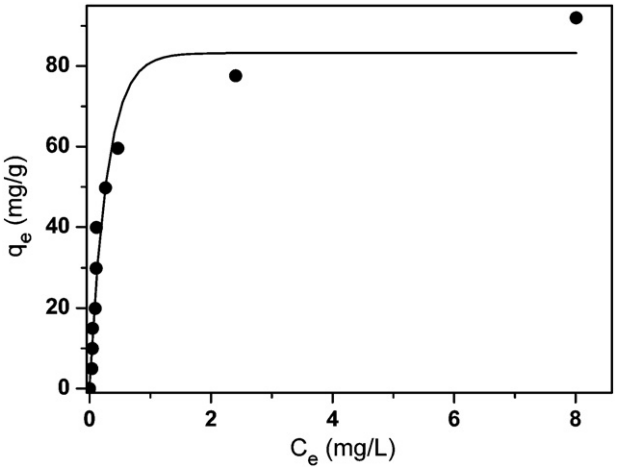

Fig. 6. The adsorption isotherm of RhB onto Fe-Ben at 298 K.

from 10 mg/L to 50 mg/L, but increased with the increasing of the dosage of adsorbent from 0.075 g/L to 0.50 g/L. The better adsorption of RhB with lower initial concentration onto Fe-Ben of the settled dosage could be attributed to the larger amount of available unoccupied binding sites on the surface of Fe-Ben [25]. Increasing the dosage of adsorbent at a fixed dye concentration provided more available adsorption sites for dye [21], so the adsorption of RhB onto Fe-Ben is better with higher dosage.

The adsorption kinetics of RhB follows the pseudo-second-order adsorption kinetic model much better than the pseudo-first-order adsorption kinetic model under different initial concentration of adsorbate and different adsorbent dosage, which is coincident with the adsorption of RhB onto montmorillonite [1] or other basic dyes onto clay adsorbents [21,26]. According to the pseudo-second-order adsorption kinetic model, the adsorption capacities and the kinetic constants were listed in Table 3. The experimental results showed that intraparticle diffusion kinetic was also involved in the adsorption process of RhB onto Fe-Ben and the intraparticle diffusion kinetic constant was also listed in Table 3. It can be seen that the adsorption capacity and the intraparticle diffusion kinetic constant of RhB increased but the adsorption kinetic constant decreased when the initial concentration of RhB increased from 10 mg/L to 50 mg/L. With the increasing of the dosage of adsorbent, the adsorption capacity and the intraparticle diffusion kinetic constant of RhB decreased whereas the adsorption kinetic constant increased.

3.4. Adsorption isotherm of RhB

The adsorption isotherm of RhB was investigated at 298 K for the design of adsorption systems. In this study, the Langmuir isotherm model and the Freundlich isotherm model were used to fit the experimental data of adsorption equilibriums of RhB onto the Fe-Ben.

Langmuir isotherm model is a monolayer adsorption model, which can be expressed as Eq. (4) or Eq. (5):

$$\frac{C_e}{q_e} = \frac{1}{q_m K_L} + \frac{C_e}{q_m} \quad (4)$$

$$\frac{1}{q_e} = \frac{1}{C_e q_{max} K_L} + \frac{1}{q_{max}} \quad (5)$$

where C_e is the equilibrium concentration of adsorbates in the solution (mg/L), q_e is the equilibrium adsorption amount of adsorbates (mg/g), q_m is the monolayer adsorption capacity of adsorbents for adsorption of adsorbates in the experiments (mg/g), and K_L is the Langmuir adsorption equilibrium constant (L/mg). The q_m and K_L can be determined by the intercept and the slope of the linear plot of C_e/q_e versus C_e, respectively.

Different from Langmuir isotherm, Freundlich isotherm is characterized by a heterogeneity factor of $1/n$, describing reversible adsorption, and is not restricted to the formation of the monolayer. Freundlich equation can be expressed as Eq. (6).

$$q_e = K_F C_e^{1/n} \quad (6)$$

where q_e is the equilibrium adsorption amount of adsorbates (mg/g), K_F is the Freundilich adsorption equilibrium constant ((mg/g)(mg/L)^n), C_e is the equilibrium concentration of adsorbates in the solution (mg/L), $1/n$ is the heterogeneity factor. Eq. (6) can be rearranged in a linear form as Eq. (7). K_F can be determined by the intercept of $\ln q_e$ versus $\ln C_e$.

$$\ln q_e = \ln K_F + \frac{1}{n} \ln C_e \quad (7)$$

Table 3
Pseudo-first-order and pseudo-second-order adsorption kinetic parameters for RhB onto Fe-Ben.

		Pseudo-first-order kinetic			Pseudo-second-order kinetic			Intraparticle diffusion kinetic		
		q_1 (mg/g)	k_1 (min^{-1})	R^2	q_2 (mg/g)	k_2 (10^{-3} g/mg min)	R^2	k_p (mg/g min$^{1/2}$)	C (mg/g)	R^2
RhB C_0 (mg/L)	10	40.16	23.33	0.960	40.23	14.06	0.999	0.74	33.14	0.841
	20	79.18	38.37	0.996	79.43	5.76	0.999	1.67	63.20	0.859
	30	108.11	29.01	0.914	113.12	1.54	0.998	4.22	68.99	0.980
	40	134.95	46.13	0.857	140.25	1.54	0.999	4.51	93.64	0.966
	50	160.26	43.29	0.929	166.94	1.08	0.998	6.14	103.14	0.975
Dose (g/L)	0.075	136.61	17.25	0.953	152.44	0.27	0.982	11.25	19.05	0.971
	0.15	92.25	4.60	0.960	96.43	1.55	0.998	3.99	54.40	0.971
	0.25	79.18	2.06	0.996	79.43	5.76	0.999	1.67	63.20	0.859
	0.50	39.75	0.05	0.970	39.75	614.59	1	0.02	39.53	0.747

Nomenclature: q_1 and q_2: the equilibrium adsorption capacities according to pseudo-first-order kinetic and pseudo-second-order kinetic models, respectively (mg/g); k_1: pseudo-first-order rate constant of adsorption (1/min); k_2: pseudo-second-order rate constant of adsorption (10^{-3} g/mg min); R^2: relative coefficient.

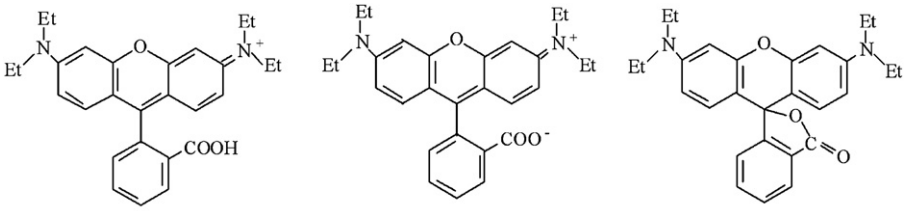

Fig. 7. Different structures of RhB.

Table 4
Langmuir and Freundilich model parameters for RhB onto Fe-Ben.

Langmuir model		Freundilich model	
$R^2 = 0.9613$		$R^2 = 0.8540$	
q_{max} (mg/g)	K_L (L/mg)	K_F ((mg/g)(mg/L)^n)	n
98.62	3.63	57.1	2.06

Fig. 6 shows the adsorption isotherm of RhB onto Fe-Ben. Table 4 summarizes the parameters for two isotherm models from the experimental results. It can be seen that the adsorption isotherm of RhB fits Langmuir isotherm model much better than Freundlich isotherm model, which can be ascribed to the effective monolayer chemisorption of RhB onto Fe-Ben. According to the Langmuir isotherm model, the adsorption equilibrium constant (K_L) for the adsorption of RhB onto Fe-Ben was 3.63 L/mg and the monolayer adsorption capacity (q_m) was 98.62 mg/g. Since Fe-Ben can adsorb RhB easily and quickly at room temperature, the dependence of adsorption of RhB onto Fe-Ben on the temperature was omitted in this paper.

3.5. Adsorption mechanism of RhB

Rhodamine B is a kind of a xanthene dye (Fig. 7). The solvents, its concentration, pH value of the solutions and the surface properties of the adsorbents significantly influence the properties of RhB.

RhB forms three kinds of protonated species with different charges: the zwitterion ($RhB^{\pm}$) and the positively charged species, $RhBH^+$ and $RhBH_2^{2+}$ [23,27]. They respectively predominate at pH values >4.0, in the pH range 1.0–3.0 and pH < 1.0 [27,28]. The increase in competition for adsorption sites by H^+ [1] could be present at much lower pH value of the reaction solution, which leads to lower adsorption capacity of RhB onto Fe-Ben at pH 3.0 than that at pH 5.0. The basic form and lactone form of RhB in the solutions of higher pH values are predominant, which are unfavorable for their adsorption onto adsorbents [1,22]. Thus, pH 5.0 is the optimal pH value for the adsorption of RhB onto the Fe-Ben.

Since there was little leaching of iron from Fe-Ben under different pH, it can be deduced that Fe-Ben is very stable, which can be further used as a promising catalyst to degrade and mineralize organic contaminants [29,30]. The research on the adsorption of RhB onto Fe-Ben might be favorable for investigating the catalytic degradation of RhB on Fe-Ben in the future.

4. Conclusions

The iron-pillared bentonite can be prepared at room temperature and it is a more effective adsorbent for removal of RhB than the natural bentonite. The specific surface area of bentonite increased greatly after iron pillaring. The pH value of the reaction solution significantly influences the adsorption of RhB onto Fe-Ben and pH 5.0 was found to be the most favorable for the adsorption of RhB onto the Fe-Ben through acid-base chemisorption. The adsorption capacity of RhB onto Fe-Ben increased when increasing the initial concentration of RhB. The work provides new sight for developing novel adsorbents and catalysts to remove RhB.

Acknowledgements

This work was supported by the National Natural Science Foundation of China (Nos. 20773041 and 20907011), Postdoctoral Science Foundation of China (No. 20090450861) and Ministry of Science and Technology of China (2008AA06Z311).

References

[1] S. Eftekhari, A. Habibi-Yangjeh, Sh. Sohrabnezhad, Application of AlMCM-41 for competitive adsorption of methylene blue and rhodamine B: thermodynamic and kinetic studies, J. Hazard. Mater. 178 (2010) 349–355.
[2] J.M. Monteagudo, A. Durán, C. López-Almodóvar, Homogenous ferrioxalate-assisted solar photo-Fenton degradation of orange II aqueous solutions, Appl. Catal. B: Environ. 83 (2008) 46–55.
[3] C. Marc, S. Marc, M.M. Joachim, G. Siegmar, Degradation of reactive dyes in wastewater from the textile industry by ozone: analysis of the products by accurate masses, Water Res. 43 (2009) 733–743.
[4] A.B. dos Santos, F.J. Cervantes, J.B. van Lier, Review paper on current technologies for decolorisation of textile wastewaters: perspectives for anaerobic biotechnology, Bioresource Technol. 98 (2007) 2369–2385.
[5] T. Aarthi, P. Narahari, G. Madras, Photocatalytic degradation of Azure and Sudan dyes using nano TiO_2, J. Hazard. Mater. 149 (2007) 725–734.
[6] L. Mouloud, B. Jean-Philippe, B. Michel, B. Omar, Alginate encapsulated pillared clays: removal of a neutral/anionic biocide (pentachlorophenol) and a cationic dye (safranine) from aqueous solutions, Colloids Surfaces A: Physicochem. Eng. Aspects 366 (2010) 88–94.
[7] Y. El Mouzdahir, A. Elmchaouri, R. Mahboub, A. Gil, S.A. Korili, Adsorption of methylene blue from aqueous solutions on a Moroccan clay, J. Chem. Eng. Data 52 (2007) 1621–1625.
[8] Z. Faiza, B. Omar, B. Michel, B. Jean-Philippe, Cooperative coadsorption of 4-nitrophenol and basic yellow 28 dye onto an iron organo–inorgano pillared montmorillonite clay, J. Colloid Interface Sci. 350 (2010) 315–319.
[9] G. Abate, J.C. Masini, Adsorption of atrazine, hydroxyatrazine, deethylatrazine, and deisopropylatrazine onto Fe(III) polyhydroxy cations intercalated vermiculite and montmorillonite, J. Agric. Food Chem. 53 (2005) 1612–1619.
[10] J.Y. Feng, X.J. Hu, P.L. Yue, Discoloration and mineralization of orange II using different heterogeneous catalysts containing Fe: a comparative study, Environ. Sci. Technol. 38 (2004) 5773–5778.
[11] M. Kurian, S. Sugunan, Characterisation of the acid–base properties of pillared montmorillonites, Micropor. Mesopor. Mater. 83 (2005) 25–34.
[12] R. Sumanta, I. Ivan, H.Q. Nurul, N.B. Sati, Photo-stability of rhodamine-B/montmorillonite nanopigments in polypropylene matrix, Appl. Clay Sci. 42 (2009) 661–666.
[13] M. Slimane, H. Oualid, S. Fethi, C. Mahdi, P. Christian, Influence of bicarbonate and carbonate ions on sonochemical degradation of rhodamine B in aqueous phase, J. Hazard. Mater. 175 (2010) 593–599.
[14] P.P. Selvam, S. Preethi, P. Basakaralingam, N. Thinakaran, A. Sivasamy, S. Sivanesan, Removal of rhodamine B from aqueous solution by adsorption onto sodium montmorillonite, J. Hazard. Mater. 155 (2008) 39–44.
[15] A.A. Schilt, Analytical Applications of 1,10-Phenanthroline and Related Compounds, 1st ed., Pergamon Press, Oxford, 1969.
[16] R.A. Horch, T.D. Golden, N.A. D'Souza, L. Riester, Electrodeposition of nickel/montmorillonite layered silicate nanocomposite thin films, Chem. Mater. 14 (2002) 3531–3538.
[17] K. Dana, S. Das, S.K. Das, Effect of substitution of fly ash for quartz in triaxial kaolin–quartz–feldspar system, J. Eur. Ceram. Soc. 24 (2004) 3169–3175.

[18] M.F. Hou, H.F. Wan, T.L. Liu, Y.L. Fan, X.M. Liu, X.G. Wang, The effect of different divalent cations on the reduction of hexavalent chromium by zerovalent iron, Appl. Catal. B: Environ. 84 (2008) 170–175.
[19] D.M. Manohar, B.F. Noeline, T.S. Anirudhan, Adsorption performance of Al-pillared bentonite clay for the removal of cobalt(II) from aqueous phase, Appl. Clay Sci. 31 (2006) 194–206.
[20] J. Ojima, Determining of crystalline silica in respirable dust samples by infrared spectrophotometry in the presence of interferences, J. Occup. Health 45 (2003) 94–103.
[21] A. Gürses, Ç. Doğar, M. Yalçın, M. Açıkyıldız, R. Bayrak, S. Karaca, The adsorption kinetics of the cationic dye, methylene blue, onto clay, J. Hazard. Mater. 131 (2006) 217–228.
[22] R. Jain, M. Mathur, S. Sikarwar, A. Mittal, Removal of the hazardous dye rhodamine B through photocatalytic and adsorption treatments, J. Environ. Manage. 85 (2007) 956–964.
[23] K. Shakir, A.F. Elkafrawy, H.F. Ghoneimy, S.G.E. Beheir, M. Refaat, Removal of rhodamine B (a basic dye) and thoron (an acidic dye) from dilute aqueous solutions and wastewater simulants by ion flotation, Water Res. 44 (2010) 1449–1461.
[24] M. Doğan, Y. Özdemir, M. Alkan, Adsorption kinetics and mechanism of cationic methyl violet and methylene blue dyes onto sepiolite, Dyes Pigments 75 (2007) 701–713.
[25] D.S. Sun, X.D. Zhang, Y.D. Wu, X. Liu, Adsorption of anionic dyes from aqueous solution on fly ash, J. Hazard. Mater. 181 (2010) 335–342.
[26] E. Eren, B. Afsin, Removal of basic dye using raw and acid activated bentonite samples, J. Hazard. Mater. 166 (2009) 830–835.
[27] G. Parisi, P. Santoro, Spectrophotometric study of several rhodamines commonly used in microscopy, Boll. Sot. Ital. Biol. Sper. 58 (1982) 683–689.
[28] A.V. Deshpande, U. Kumar, Effect of method of preparation on photophysical properties of RB impregnated sol–gel hosts, J. Non-Cryst. Solids 306 (2002) 149–159.
[29] E.G. Garrido-Ramírez, B.K.G. Theng, M.L. Mora, Clays and oxide minerals as catalysts and nanocatalysts in Fenton-like reactions — a review, Appl. Clay Sci. 47 (2010) 182–192.
[30] N. Sergio, A. Mercedes, G. Hermenegildo, Heterogeneous Fenton catalysts based on clays, silicas and zeolites, Appl. Catal. B: Environ. 99 (2010) 1–26.